Temporal Patterns In Extended Systems With Stochastic Dynamics

A thesis submitted in partial fulfillment of the requirements for the award of the degree of

Master of Technology

Rakesh Pandey

School of Information Technology

Jawaharlal Nehru University

New Delhi - 110067

July 2008

Dedicated

to

My Parents

DECLARATION

I hereby declare that the work carried out in this thesis is entirely original. It was carried out by me in the School of Information Technology, Jawaharlal Nehru University, New Delhi. I further declare that it has not formed the basis for the award of any degree, diploma, membership or similar title of any university or institution.

Rakesh Pandey
Centre for Computational
Biology and Bioinformatics
School of Information Technology
Jawaharlal Nehru University
New Delhi, INDIA
2008

Indira Ghosh
Dean
School of Information Technology
Jawaharlal Nehru University
New Delhi, INDIA

Ramakrishna Ramaswamy
Thesis Supervisor
Centre for Computational
Biology and Bioinformatics
School of Information Technology
Jawaharlal Nehru University
New Delhi, INDIA

Acknowledgment

First of all I would like to express, my sincere and deepest gratitude to my supervisor Prof. Ram Ramaswamy. A few lines are too short to make a complete account of my deep appreciation for him. His enthusiastic and dedicated view of research inspired me for research. He provided freedom and very friendly environment, which helped me to complete this study. He introduced me the study of Dynamical systems, especially the dynamics of gene regulatory circuits.

I am deeply grateful to Mr.Amitabha Nandi, a graduate student of my supervisor. Without his help it was very difficult to complete this work.

I am also very grateful to Prof. Alok Bhattacharya and Prof. Indira Ghosh to make available whatever resources required to carry out this study. I would like to acknowledge Dr. Naidu Subbarao, Dr. A. Krishnamachari, Dr. Narinder Singh Sahni, and Dr. Andrew M Lynn, Dr. Supratim Sengupta and Dr. Pradipta Bandyopadhyay for their suggestions and academic help.

I owe sincere thanks to staff of school for their support.

I would like to acknowledge my seniors, PhD students and colleagues Rakesh Tewari, Rhul, Sarbashis Das and Md. Rehan for their constant support and motivation to carry out this work.

I owe great gratitude for my family especially for my father who always motivate me for education and always ready to do whatever was required for that. Love and blessing of my mother and sister have been the greatest strength of my life. I also thankful to Priyanka who motivate and help me during this work.

Last but most, I bow down before the ALMIGHTY.

Rakesh

Rakesh Pandey

Contents

Chapter 1

Introduction

Many physiological functions and activities such as sleep, body temperature, alertness, neurotransmitter levels etc have rhythmic properties. Numerous examples are known: the liver is more active during the night than it is during the day, menstrual cycles have a period of about 28 days, and immunity and iron concentrations in the blood reach low levels during menstruation and high levels during ovulation. The sleep-inducing hormone *Melatonin* is secreted in response to the darkness of night and is therefore also periodic. Biological rhythms can have period lengths ranging from fractions of seconds to decades. These rhythms are subdivided into Ultradian, Circadian and Infradian. Circadian from the Latin *circa diem* or about one day, indicates that the cycle occurs about once a day. If the period of rhythms is less than 20 hr then it is termed as Ultradian, and if more than 30 hr Infradian. Ultradian include electrical firing of neurons (period in the millisecond range), heart beats (period $\approx$ 1 s in humans), sleep episodes (period $\approx$10 min in rats, 90 min in humans), yeast respiration (period $\approx$ 40 min), somite formation during vertebrate embryogenesis (period $\approx$ 20 min in zebrafish, 90 min in chicken), and foraging in the common vole *Microtus avails* (period $\approx$ 150 min). Similarly, infradian rhythms include such diverse cycles as the female estrus cycle (period $\approx$ 4-5 days in mice, 28 days in humans), circannual mating rhythms (period $\approx$ 1 year), and emergence cycles of cicada (period $\approx$ 13-17 years) [1].

To explore Biological rhythms at the molecule level, one approach is to build synthetic oscillators de novo. The first synthetic oscillator constructed by Elowitz and Leibler was a ring oscillator [2] termed *Repressilator*. This was composed of three transcriptional repressor systems that are not part of any natural biological clock, each of which regulates the expression of another repressor: Repressor 1 (LacI) repressed the expression of repressor 2 (TetR) and similarly repressor 2 repressed the expression of repressor 3 (λcI). Finally, repressor 3 repressed the expression of repressor 1 (LacI). This leads to oscillations in green fluorescent protein as a readout of its state in individual cells. The resulting oscillations, with typical periods of hours, are slower than the cell-division cycle, so the state of the oscillator has to be transmitted from generation to generation [2].

There are other well known models as well: one design is [3] based on a Lotka-Volterra type system with a predator (lacI)-prey(glnG) pair. The regulators exhibit oscillation, with time period from 10 to 20 hr. A positive regulator (GlnG) activates its own expression, and the expression of the repressor (LacI). The repressor LacI represses the expression of the activator: the activator can thus be considered as a prey that "feeds into" the predator LacI, which decreases the population of the prey.

A third example, termed *Metabolator*, has been designed and constructed by Fung et al. [4]. This synthetic oscillator is incorporated into the central metabolism of the host organism; the conceptual design of this gene metabolic oscillator consists of a flux-carrying network with two interconverting metabolite pools (M_1 and M_2) catalyzed by two enzymes E_1 and E_2, the expressions of which are negatively and positively regulated by M_2, respectively. In the first stage, when the level of M_2 is low, E_1 is expressed and E_2 is not. A high input metabolic flux rapidly drives M_1 to M_2. Accumulation of M_2 represses E_1 and up regulates E_2. When the backward reaction rate exceeds the sum of the forward reaction rate and the output rate, the level of M_2 decreases and the M_1 level increases. E_1 is then expressed again and E_2 is degraded, returning the circuit to the first stage. On the other hand, if the input flux is low, M_2 does not accumulate sufficiently fast to cause a large swing in gene expression, and a stable steady state can

be reached [4].

In the present study I investigate the stochastic dynamics of such model biological oscillators using the Gillespie stochastic simulation algorithm [8]. As a model I study a gene regulatory circuit which shows circadian oscillation [5] and a model chemical system the Brusselator [8]. The circadian model is based on common positive and negative control elements found experimentally [6]. Futher I explore the nature of synchronization when two or more stochastic oscillators are coupled by microscoping coupling mechanism [30]. Synchronization, which may be a desired phenomenon in synthetic biological networks, is a well studied behavior of dynamical systems in physical sciences, but less understood in biology. In analysis of gene regulatory networks, separation of time scale is a major difficulty. These separations are typically fast reactions (dimerization, protein-DNA binding/unbinding) and slow reactions (transcription, translation, degradation). Many studies have been done for reduced description of these systems using the idea of quasiequilibrium for fast processes compared with the slow dynamics [9]. These approaches have implicitly assumed that all of the reactions (fast and slow) are Markovian processes obeying Poissonian statistics. But transcriptional and translational processes are not just slow but also are compound multistage reactions involving the sequential assembly of long molecules. Therefore by central limit theorem, these processes should obey Gaussian statistics with a certain characteristic mean delay time [29]. When delay is small compared to other time scales which are characterizing the system, it is safe to ignore that in simulations but in the case, when time delay is of the order of other processes or longer it is necessary to take that into account. To take into account the non-Markovian nature of dynamics due to time delay biochemical reactions, I use the modified Gillespie Algorithm [29]. Nature of synchronization vary as a function of delay time, in phase, antiphase or out of phase. Further I study a particular coupling topology in which three oscillators are bidirectionally coupled: oscillators 1 and 3 are coupled indirectly via oscillator 2. We observe that oscillators 1 and 3 are phase synchronized though they are not directly coupled, such phenomenon is termed as "relay synchronization". For different combinations of delay time and coupling strength, one

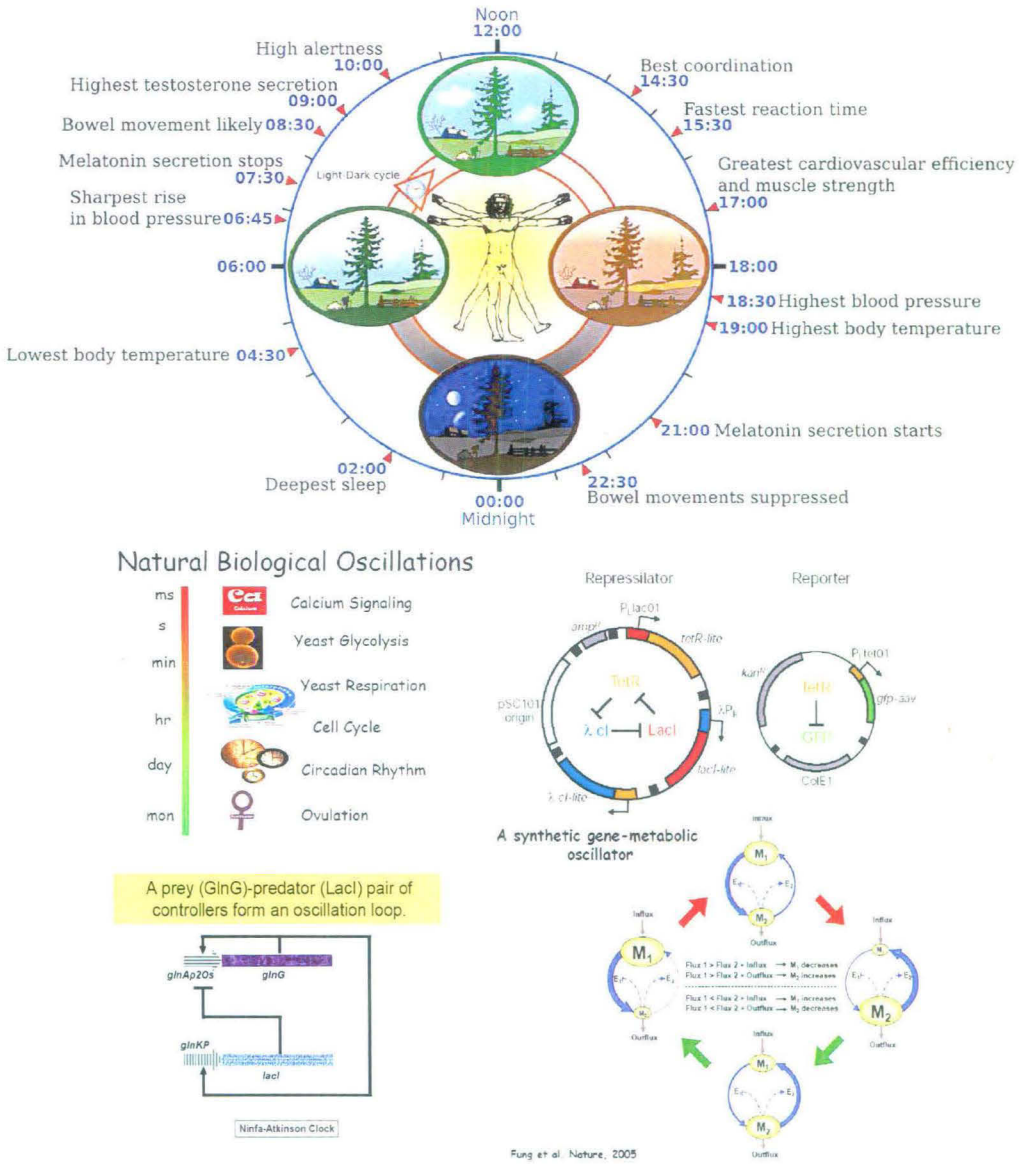

Figure 1.1: Natural and Synthetic oscillators

can find regimes where either oscillator 2 is in antiphase or out of phase to 1 and 3 which are phase synchronized. With the help of coupling mechanism [30], I study the nature of synchronization in ensembles of extended systems composed of stochastic oscillators. Incorporating relay synchronization and considering the circadian oscillator at each node I study simple network motifs [36]. Structure of my thesis is as follows.

In chapter 2, I discuss the type of formalism to study the dynamics of the biological oscillators, namely deterministic and stochastic formalism. In stochastic formalism I discuss different formalism like the master equation approach, stochastic simulation algorithm, improvements to stochastic simulation algorithm, and chemical langevin equation approach. I also discuss modified Gillespie stochastic simulation algorithm which take time delay into account.

In chapter 3, firstly I discuss the coupling mechanism: direct coupling and exchange coupling and their application to the Brusselator and Circadian oscillator. Then I posted the results of stochastic simulation of single Brusselator, circadian oscillator, coupled Brusselator and circadian oscillator. Further I discuss the case of time delay and relay synchronization simulation results. Considering circading oscillator as each node I discuss the simple network motifs. Results are shown for linear chains, triangular and square motifs as examples of mentioned network topology.

In chapter 4, I conclude my present study.

Chapter 2

Dynamics

Study of the dynamical behavior of biological systems is necessary to understand the complexity of such systems at the cellular level. At this level the dynamics is essentially the kinetics of the biochemical reactions. There are two mathematical formalism describing the chemical kinetics, the deterministic and stochastic approaches. The deterministic approach considers the time evolution as a continuous and predictable process whereas the stochastic approach regards the time evolution as a random process. In the deterministic approach, one integrates set of coupled, ordinary differential equations the *reaction-rate equations.* In the stochastic approach the evolution is governed by the *Master Equation.*

2.1 Deterministic Formalism

In macroscopic view of bio-chemical reactions one makes the assumptions that the biochemical reactions involve large numbers of molecules of the involved reacting species and the changes of concentration are continuous. The evolution follows from the chemical rate laws which governs the concentrations of the reacting species. These have the general form

$$\begin{aligned} \frac{dX_1}{dt} &= f_1(X_1, \ldots, X_N) \\ \frac{dX_2}{dt} &= f_2(X_1, \ldots, X_N) \\ \frac{dX_N}{dt} &= f_N(X_1, \ldots, X_N), \end{aligned} \tag{2.1}$$

where the X's represent concentrations and the f's are nonlinear functions.

Solving these equations for $\{X_i, ...X_N\}$ with the help of prescribed initial conditions is analytically possible only for the small systems. For systems with large number of species one has to solve this numerically. There are many methods a few of which are

- Euler Method
- Runge Kutta Methods
- Adam-Moulton Gear Method

There are various tools for sensitivity analysis, equilibrium analysis and bifurcation analysis to gather more information of the systems and a variety of software packages especially developed for deterministic simulation and analysis of biochemical reaction systems, such as DBsolve [10], GEPASI [11], KINSIM [12], MIST [13], KINSOLVER [14], PLAS [15], ECELL [16] and Cellware [17] have become available.

2.2 Stochastic Formalism

When the concentrations of the reacting species are low conventional deterministic chemical kinetics may not be appropriate [18, 19]. The stochastic approach provides a more realistic view of the dynamics of the system. Since in thermal equilibrium (not necessarily in chemical equilibrium) collisions in a system of molecules occur randomly.

The temporal behavior of a spatially homogeneous mixture of molecular species can studied by different approaches, Master Equation or numerically via the Stochastic Simulation Algorithm [8] or the Chemical Langevin Equation [20].

Consider a mixture of the N molecular species $S_1, ..., S_N$ chemically interacting at some constant temperature T in volume V through M reaction channels $R_1, ..., R_M$. Then the dynamical system is specified by the vector

$$\mathbf{X(t)} = (X_1(t), X_2(t), \ldots, X_N(t)) \tag{2.2}$$

where $X_i(t)$ is the number of S_i molecules in the system at time t ($i = 1, ..., N$). Any reaction channel R_j can be mathematically characterized by two quantities, the state vector ν_j, whose ith component is ν_{ji}: the change in the number of S_i molecules produced by one R_j reaction and the propensity function a_j which is defined as follows

$$\begin{aligned} a_j(x)dt \quad = \quad & \text{the probability, given} X(t) = x \text{ that one reaction} \\ & R_j \text{ will occur somewhere inside } V \text{ in infinitesimal} \\ & \text{time interval } (t, t+\tau) \text{ where } (j = 1, ..., M). \end{aligned} \tag{2.3}$$

It has been shown that Eq. 2.3 leads directly to the formulation of the chemical master equation [21], and also to an approximating Chemical Langevin equation and Fokker-Planck equation [20] .

For biomolecular rection the function a_j is found to have the following mathematical form [21]

$$a_j(x) = c_j h_j(x) \tag{2.4}$$

where c_j is the specific probability rate constant for channel R_j, defined so that $c_j dt$ gives the probability that a randomly chosen pair of R_j reactant molecules will react in the next infinitesimal time interval dt. The reaction constants k_j's, are related to the c_j's through

$$c_j = k_j V^{1-\alpha_j} \tag{2.5}$$

where α_j is the sum of stoichiometric coefficients of a particular reaction. The function $h_j(x)$ in equation Eq. 2.4 is defined to be the number distinct combinations of R_j reactant molecules available in the state x. So, if R_1 were the reaction $X_1 + X_2 \rightarrow 2X_1$ we would have $a_1 = c_1 x_1 x_2$, and if R_2 were the inverse of that reaction we would have $a_2 = c_2 x_1(x_1 - 1)/2$

2.2.1 Master Equation Formalism

The traditional way to study the time evolution of a spatially homogeneous mixture of molecular species is by examining the probability function,

$$P(x, t|x_0, t_0) \equiv \text{Prob}(X(t) = x, \text{ given that} X(t_0) = x_0). \tag{2.6}$$

The time evolution of this function, obeys a master equation,

$$\begin{aligned} P(x, t + dt|x_0, t_0) &= P(x, t|x_0, t_0) \times \left[1 - \sum_{j=1}^{M} a_j(x)dt\right] \\ &\quad + \sum_{j=1}^{M} \left[P(x - \nu_j, t|x_0, t_0)a_j(x - \nu_j)dt\right], \end{aligned} \tag{2.7}$$

where the first term represents the probability that the system will be in the state x at time t, and then remains in that state in $(t, t + dt)$ and the second term gives the probability that the system is one R_j reaction removed from the state x at time t, and then undergoes an R_j reaction in $(t, t + dt)$. By algebraic rearrangement and taking the limit $dt \rightarrow 0$, one can get the chemical master equation.

$$\begin{aligned} \frac{\partial P(x, t|x_0, t_0)}{\partial t} &= \sum_{j=1}^{M} \left[a_j(x - \nu_j)P(x - \nu_j, t|x_0, t_0)\right] \\ &\quad - a_j(x)P(x, t|x_0, t_0) \end{aligned} \tag{2.8}$$

2.2.2 Stochastic simulation Algorithm

It is difficult to solve the chemical master equation for the probability density function $X(t)$ and therefore it is necessary to use numerical methods to get trajectories of $X(t)$. A key to generating the simulated trajectories of $X(t)$ is the probability function $p(\tau, j|x, t)$, the *next-reaction density function* [23], defined as

$$\begin{aligned} p(\tau, j|x, t)d\tau \quad \equiv \quad & \text{Probability, given} X(t) = x, \text{ the next} \\ & \text{reaction in } V \text{ will occur in the infinitesimal} \\ & \text{time interval } [t+\tau, t+\tau+d\tau], \\ & \text{and will be an } R_j \text{ reaction.} \end{aligned} \tag{2.9}$$

Since $\sum_j a_j(x)dt$ is the probability that some reaction will occur in the next interval dt, with the help of the elementary theory of probability one can show that $\exp(-\sum_j a_j(x)\tau)$ is the probability that a time τ will pass by without any reaction occurring. This leads, in straight forward manner, to

$$p(\tau, j|x.\, t)d\tau = a_j(x)\exp\left(-\sum_{k=1}^{M} a_k(x)\tau\right) (0 \leq \tau < \infty; j = 1, ..., M) \tag{2.10}$$

This formula is the basis for the *stochastic simulation algorithm*, in which Monte Carlo techniques are used to generate random pairs (τ, j). We draw two random numbers r_1 and r_2 from a uniform distribution in the unit interval, and take

$$\begin{aligned} \tau \quad &= \quad \frac{1}{a_0(x)}\ln(\frac{1}{r_1}) \\ j \quad &= \quad \text{the smallest integer satisfying} \\ & \quad \sum_{j'=1}^{j-1} a_{j'}(x) < r_2 a_0(x) \leq \sum_{j'}^{j} a_{j'}(x), \end{aligned} \tag{2.11}$$

where $a_0(x) = \sum_{j=1}^{M} a_j(x)$.

In brief the algorithm can be summarized as follows:

- Step (0). Initialize the time $t = t_0$ and the system state $x = x_0$.
- Step (1). With the system in state x at time t, evaluate all the $a_j(x)$ and their sum $a_0(x)$.
- Step (2). Generate values for τ and j using Eq. 2.11 (or their equivalent).
- Step (3). Effect the next reaction by replacing $t \leftarrow t+\tau$ and $x \leftarrow x+\nu_j$.
- Step (4). Record (x, t) as desired. Return to Step 1, or else end the simulation.

2.2.3 Improvements to the stochastic Simulation Algorithm

The above mentioned Algorithm is known as the *Direct-Method.* A variation of the stochastic simulation algorithm (SSA) [23] which differs only in generating values of τ and j is known as *first reaction method.* Here one generates M random numbers $r_1, ..r_M$ from the the unit-interval uniform distribution, computes

$$\begin{aligned} \tau_{j'} &= 1/a_{j'}(x)\ln(1/r_{j'}) \\ \tau &= \text{smallest of the}\{\tau_{j'}\} \text{ and} \\ j &= \text{the index of the smallest of the}\{\tau_{j'}\} \end{aligned}$$

Heuristically, $\tau_1 ..\tau_M$ are putative times to the next firings of the respective reaction channels. however, we accept only the earliest of those and discard the rest. It can be proved [23] that this procedure, like the direct method, generates values for τ and μ in exact accord with the joint density function. However, if the system has many reaction channels, this method will be computationally less efficient than the direct method [24].

Three situations can cause an increase of computational effort in the Gillespie algorithm. The conditions are as follows [25],

- Increase in the number of reaction channels.
- Increase in the number of molecules of the species.
- Faster reaction rate of the reaction channels.

These conditions decrease the time step of each iteration thus forcing the algorithm to run for larger number of iterations to simulate a given experiment.

As a result, disparities occurs in the time scale of reaction channels in the system, which is similar to stiffness problem in ODE method. In the stochastic algorithm whenever the complexity of the system increases, either through any of the above mentioned reasons, the algorithm takes small τ to maintain the exactness of the simulation i.e. algorithm requires shorter time step to capture the dynamics of the system and therefore computation will slow down significantly.

Gibson and Bruck [26] enhanced the Gillespie first reaction method for large N and M in *next-reaction method.* They use indexed binary tree priority queue to save the putative next firing times of all reaction channels. Although the next-reaction method can be significantly faster than the direct method, it is much more challenging to code [24].

In 2001, Gillespie [27] devised a τ -leap method which provides significant gain in the computational speed, with an acceptable loss in accuracy. He proposed that it is sometimes unnecessary to obtain so much detail from the simulation, one may like to have information that how many of each reaction channels are fired in a certain time interval rather than to find out which reaction happens at which time step. It is possible to get substantial gain in the computational speed, if the time interval is large enough for many reactions to happen. Gillespie describes that it is possible to approximate the Poisson distribution with a normal distribution at the cost of accuracy [27] and has provided different mechanisms for selecting τ [27].

2.2.4 Chemical Langevin Equation

The master equation is able to describe accurately the stochastic dynamical behavior of a well-stirred mixture of N molecular species that chemically interact through M reaction channels. When two explicit dynamical conditions [20] are satisfied, the microphysical premise from which the chemical master equation is derived leads directly to an approximate time-evolution equation of the Langevin type.

The two conditions are:

- τ to be small enough that change in the state during $(t, t+\tau)$ will be so slight that none of the propensity functions changes its value appreciably.
- τ is large enough that the expected number of occurrences of each reaction channel R_j in $(t, t+\tau)$ be much larger than 1.

With these assumptions one can obtain [20] the following expression,

$$\begin{aligned} X_i(t+dt) &= X_i(t) + \sum_{j=1}^{M} \nu_{ji} a_j(X(t))dt \\ &\quad + \sum_{j=1}^{M} \nu_{ji} a_j^{1/2}(X(t))\mathcal{N}_j(t)(dt)^{1/2} \end{aligned} \tag{2.12}$$

where $(i = 1, ..N)$ and $\mathcal{N}_j(t)$ is unit normal random variable. This equation has the canonical form of a standard Langevin equation for multivariate continuous Markov process. So equation Eq. 2.12 can implies the equivalent white noise form Langevin equation [20].

$$\begin{aligned} \frac{dX_i(t)}{dt} &= \sum_{j=1}^{M} \nu_{ji} a_j(X(t)) + \sum_{j=1}^{M} \nu_{ji} a_j^{1/2}(X(t))\Gamma_j(t) \\ &\quad \text{where } (i = 1, ..N) \end{aligned} \tag{2.13}$$

The $\Gamma_j(t)$'s are temporally uncorrelated, statistically independent Gaussian white noise. Eq. 2.13 also implies the singly conditioned density function for $X(t)$ obeys the (forward) Fokker-Planck Equation [20].

2.3 Time delay Gillespie algorithm

When dealing with time delayed channels Bratsun et al. [29] devised a modification of the Gillespie scheme . This takes into account the non Markovian nature of the dynamics when time delay is present. In short, the algorithm is as follows:

- Step (1) Input initial values for initial state $X = (X_1, ..X_N)$, set time $t = 0$, and reaction counter $i = 1$.
- Step (2) Compute propensities of M reactions $a_j (j = 1, \ldots, M)$.
- Step (3) Generate uniform random numbers $r_1, r_2 \in \{0, 1\}$.
- Step (4) Compute the time interval until the next reaction $\triangle t_i = -\ln r_1 / \sum_j a_j$.
- Step (5) Check whether there are delayed reactions scheduled within time interval $[t, t + \triangle t_i]$. If *yes*, then Steps 2 to 4 are ignored, time t advances to the time t_d of the next scheduled delayed reaction, X states are updated according to the delayed reaction channel, and counter is increased $i = i + 1$. Proceed to *step* 2. If *no*, go to Step 6.
- Step (6) Find the channel of the next reaction j. take j, integer for which $\sum_{j'=1}^{j-1} a_{j'} < r_2 a_0 \leq \sum_{j'=1}^{j} a_{j'}$ where $a_0 = \sum_{j=1}^{M} a_j$ is the total propensity.
- Step (7) If the selected reaction is not delayed, update X according to the R_j, update time $t = t + \triangle t_i$ and increase counter $i = i + 1$. If the selected reaction is delayed, update is postponed until time $t_d = t + \tau$. Go to Step 2.

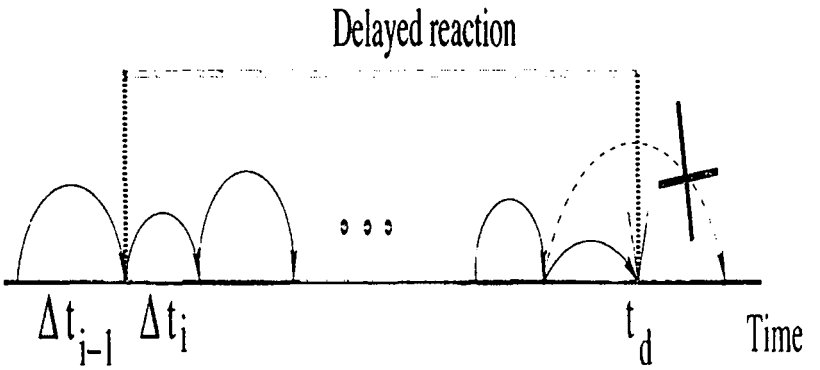

Figure 2.1: Illustration of the modified Gillespie algorithm for normal and delayed reactions.

Chapter 3

Results

3.1 Coupling Mechanism and Topologies

To couple two or more stochastic oscillatory systems I use the microscopic coupling mechanism recently studied by Nandi et.al [30]. A stochastic system can be specified by a set of elementary processes which can be written in the following way [30]

$$X_i + X_j + ... \xrightarrow{c_m} X_k + X_l + ... \tag{3.1}$$

where X's are non-negative integers and it represent the number of molecules of different chemical species (represented by the subscript). c_m represents rate of the mth such channel. A configuration of the system C is a specification of the variables, $(X_1X_2.....X_N)$ [30]. The evolution of configurational probabilities [31] follows

$$\frac{dP(C,t)}{dt} = -\sum_{c'} P(C,t)W_{c\to c'} + \sum_{c'} P(C',t)\,W_{c'\to c} \tag{3.2}$$

where in standard notation [32], $P(C,t)$ is the probability of configuration C at time t and $\{W\}$ are the transition probability. To study such systems one use stochastic (Monte Carlo) simulation techniques [8].

Now consider two such identical but independent stochastic systems with the variable of the two systems being denoted by unprimed and primed quan-

tities, say. Subsequent evolution of each of the subsystems, starting with configurations C and C' will be uncorrelated. So our interest is to couple subsystems to see the correlated temporal patterns with stochastic dynamics.

In the mechanism [30], for simplicity the two subsystems, specified by the variables X and X', have similar channels. However the corresponding rates need not be identical. Then, the two coupling mechanisms are

A. Exchange coupling

In an "exchange" process variables X_i and X_i', say interconvert. This introduces additional channels

$$X_i \underset{c'}{\overset{c}{\rightleftharpoons}} X_i' \tag{3.3}$$

which serves to couple the subsystems. The other variables X_j and X_j' show synchronization behavior, depending upon the rate of interconversion (governed by c and c'). In the case when rates of exchange are equal, in the limit $c = c' \to \infty$, this reduce to the following case:

B. Direct coupling

The variables X_i and X_i' are identical; then this is essentially a "master-slave" coupling scenario, where the two subsystems share a common drive and consequently the dynamics of the remaining variables becomes correlated.

In the case of direct coupling, effectively one species X_i is common to two reaction schemes, which is not uncommon in biochemical processes. In the same way, in exchange scenario, the species X_i and X_i' can be considered different forms of each other, or the same species in different locations say in different cells. [30]

In the sections below we study two model examples where the above coupling schemes are implemented to achieve stochastic synchronization.

3.2 Brusselator

Brusselator is a chemical oscillatory system governed by the following "chemical reactions" [8].

$$\begin{aligned} A_1 &\xrightarrow{c_1} X \\ A_2 + X &\xrightarrow{c_2} Y + A_3 \\ 2X + Y &\xrightarrow{c_3} 3X \\ X &\xrightarrow{c_4} A_4 \end{aligned} \tag{3.4}$$

In the thermodynamic limit, when fluctuations are negligible, the following a set of deterministic reaction rate equations can be derived for the average concentrations of species of X and Y,

$$\begin{aligned} \frac{dx}{dt} &= c_1 - c_2 x + \frac{c_3}{2} x^2 y - c_4 x \\ \frac{dy}{dt} &= c_2 x - \frac{c_3}{2} x^2 y \end{aligned} \tag{3.5}$$

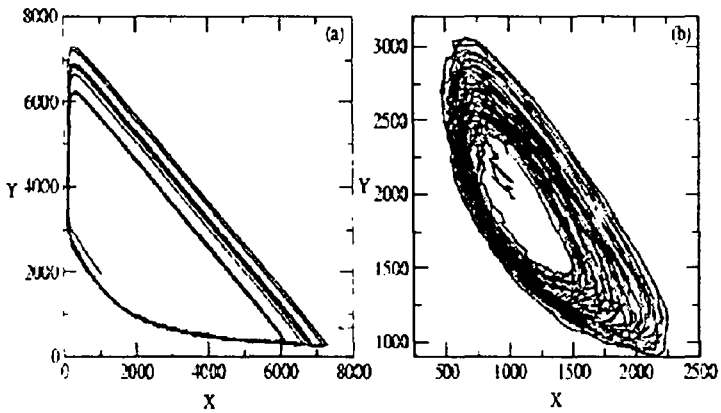

Figure 3.1: Phase portrait of single Brusselator dynamics obtained using Gillespie Algorithm . (a) Phase portrait in the low noise limit. The parameter values are $c_1 = 5000$, $c_2 = 50$, $c_3 = 0.00005$, and $c_4 = 5$ (b) Phase portrait in the high noise limit . The modified parameter values are $c_1 = 4.5 \times 5000$ and $c_4 = 4.5 \times 5$.

For suitable choices of parameters, Eq.(3.5) give a limit-cycle solution.

Simulations of Eq.(3.4), give orbits that describe a noisy limit cycle '8' as shown in Fig. 3.1 and also the variation of X an Y with time is shown in Fig. 3.2

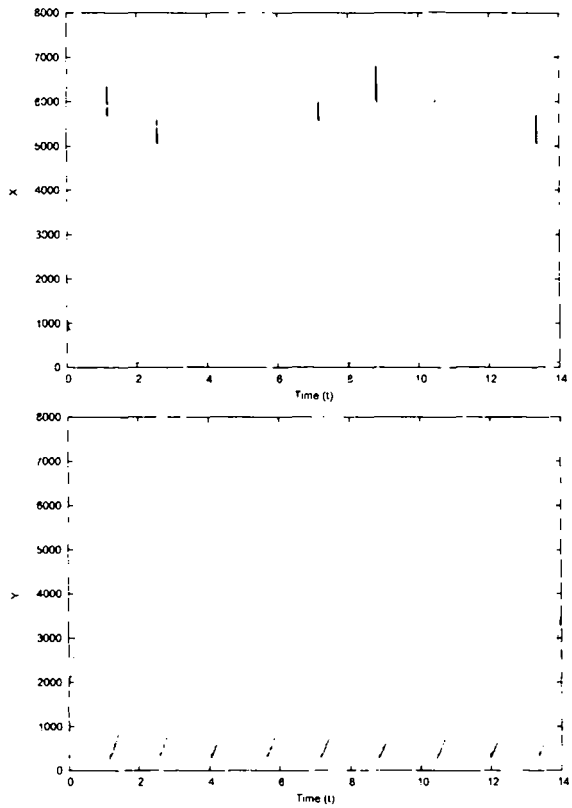

Figure 3.2: Species X and Y as a function of time. The parameter values are $c_1 = 5000$, $c_2 = 50$, $c_3 = 0.00005$, and $c_4 = 5$.

3.2.1 Direct coupling of Brusselator

Coupling the two systems through X and X' leads to synchronization of species Y and Y' as shown in Fig. 3.3. For example, in the case of direct coupling, the coupled system is represented by the following chemical reactions:

$$
\begin{aligned}
A_1 &\xrightarrow{c_1} X \\
A_2 + X &\xrightarrow{c_2} Y + A_3 \\
2X + Y &\xrightarrow{c_3} 3X \\
X &\xrightarrow{c_4} A_4 \\
A_2 + X &\xrightarrow{c_2'} Y' + A_3 \\
2X + Y' &\xrightarrow{c'3} 3X
\end{aligned}
\tag{3.6}
$$

3.2.2 Exchange coupling of Brusselator

In the case of exchange coupling the system is enlarged to

$$A_1 \xrightarrow{c_1} X \tag{3.7}$$

$$A_1 \xrightarrow{c_1'} X' \tag{3.8}$$

$$A_2 + X \xrightarrow{c_2} Y + A_3 \tag{3.9}$$

$$A_2 + X' \xrightarrow{c_2'} Y' + A_3 \tag{3.10}$$

$$2X + Y \xrightarrow{c_3} 3X \tag{3.11}$$

$$2X' + Y' \xrightarrow{c_3'} 3X' \tag{3.12}$$

$$X \xrightarrow{c_4} A_4 \tag{3.13}$$

$$X' \xrightarrow{c_4'} A_4 \tag{3.14}$$

$$X \underset{c'}{\overset{c}{\rightleftharpoons}} X' \tag{3.15}$$

Species Y and Y' as a function of time for the coupled Brusselator system is shown in Fig. 3.4.

The scheme discussed above works for coupling an ensemble of oscillators. Fig. 3.5 shows the synchronization behavior for 10 Brusselators, each oscillator being coupled to every other oscillator via exchange coupling.

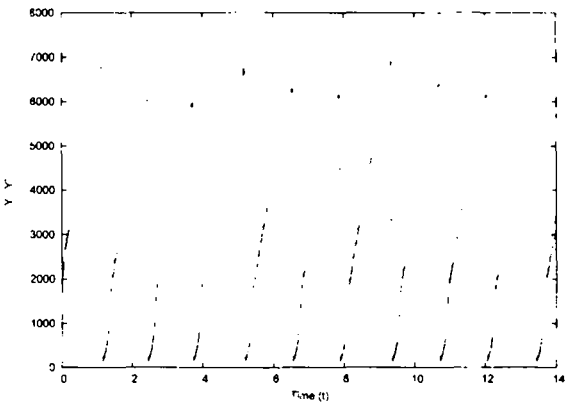

Figure 3.3: Species Y and Y' as a function of time for the coupled Brusselator system. The parameter $c_2 = 50$ differs from $c_2' = c_2 + 5$. The other parameters are $c_1 = c_1' = 5000$, $c_3 = c_3' = 0.00005$, and $c_4 = c_4' = 5$. c_1 and c_4 are taken as 2 times the given value in the case of direct coupling.

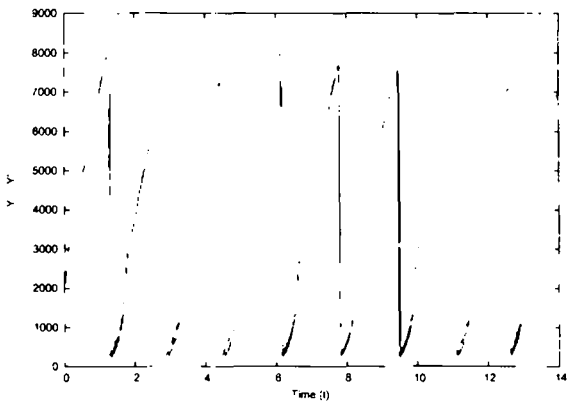

Figure 3.4: Stochastic simulation results using exchange coupling. Parameters are same as direct coupling except that in Eq. 3.15 $c = c' = 0.6$.

3.3 Circadian Oscillator

Environmental periodicity such as daily cycles of light and dark and annual cycles of changing climates and physical conditions create the necessity for organisms to develop internal time-keeping mechanisms to accurately anticipate these external changes and modify their state accordingly [7]. In particular, a wide range of organisms, as diverse as Cyanobacteria and mammals, have evolved circadian rhythms with a period of about 24 hr. The main characteristic is the presence of intracellular transcription regulation

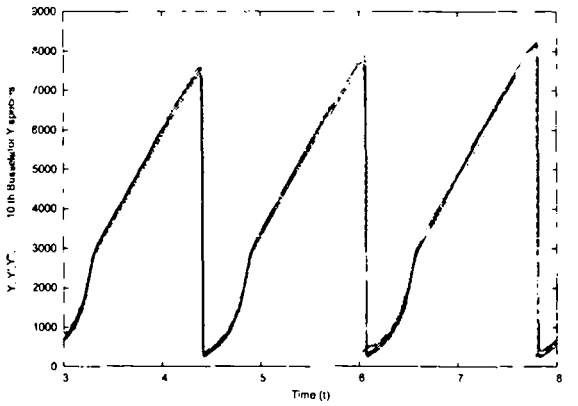

Figure 3.5: Synchronized behavior of 10 distinct Brusselator systems, namely, where all the parameters differ. I use a mean-field (all-to-all) coupling with $c = 0.9$.

networks with a set of clock elements that give rise to stable oscillations in gene expression. A positive element activates genes coupled to the circadian clock. It simultaneously promotes the expression of a negative element, which in turn represses the positive element. The cycle completes itself upon degradation of the negative element and re-expression of the positive element [5].

A crucial feature of circadian clocks is the ability to maintain a constant period over a wide range of internal and external fluctuations [7]. Such robustness ensures that the clock runs accurately and triggers the expression of clock-dependent genes at the appropriate time of the day.

3.3.1 Gene Regulatory Circuit of the Circadian Oscillator

To study the dynamics of circadian clock, I use the model that has quantitatively been studied in the context such as *Noise-Resistance In Genetic Oscillators* [6]. For a single circadian oscillatory system, Gillespie stochastic algorithm is used, and results are shown in Fig. 3.8.

When two such circadian oscillators are coupled, the biochemical network for the case of *direct coupling* is shown in Fig. 3.6. This is a system of two genetic circuits that share a single activator which binds to the two promoter

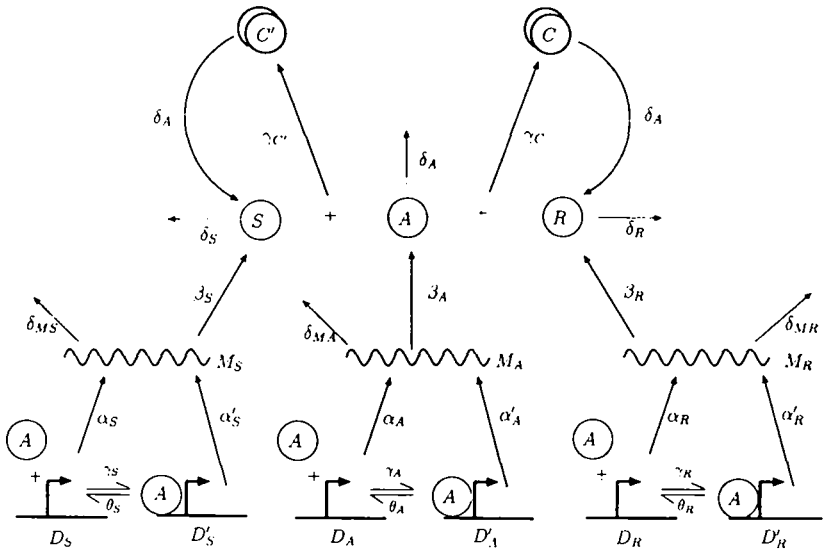

Figure 3.6: Biochemical network of the extended circadian oscillator model. D'_A and D_A denote the number of activator genes with and without A bound to its promoter respectively; similarly, D'_R D_R and D'_S D_S refer to the two repressor promoter driven by the common promoter A; M_A, M_R and M_S denote mRNA of activator A, and repressors R and S; C and C' corresponds to the inactivated complex formed by A and R, and A and S, respectively. The constants α and α' denote the basal and activated rates of transcription, β denotes the rate of translation, δ denotes the rates of spontaneous degradation, γ denotes the rates of binding of A to the other components. and θ denotes the rates of unbinding of A from those components. The values of the parameters are given in Table I. The initial conditions are $D_A = D_R{=}D_S{=}1$ mol, $D'_A = D'_R{=}D'_S{=} M_A{=}M_R{=}M_S{=}A{=}R{=}C{=}0, S{=}1, C' = 1$. The cell has a single copy of the activator and repressor genes: $D_A + D'_A = D_R + D'_R = D_S + D'_S{=}1$ mol, and the volume is assumed to be unity. .

Parameters	Values
α_A, α'_R, β_A, θ_A	50 h^{-1}
α'_A	500 h^{-1}
α_R	0.01 h^{-1}
α_S	α_R+0.001 h^{-1}
α'_S	α'_R+5 h^{-1}
β_R	5 h^{-1}
β_S	β_R+0.5 h^{-1}
δ_{MA}	10 h^{-1}
δ_{MR}	0.5 h^{-1}
δ_{MS}	δ_{MR}+0.05 h^{-1}
δ_A,	1 h^{-1}
γ_A,γ_R,γ_S	1 mol^{-1} h^{-1}
δ_R	0.2 h^{-1}
δ_S	δ_R+0.2 h^{-1}
γ_C, γ'_C	2 mol^{-1} h^{-1}
θ_R, θ_S	100 h^{-1}

Figure 3.7: Parameter values for the coupled circadian oscillator which is shown in Fig. 3.6

sites of represser proteins R and S. For the case of exchange coupling the circuit will be different from the Fig. 3.6 in the sense that the circuit [5] will be essentially doubled.

Each individual circuit gives stochastic oscillations in the number of repressor molecules. When the two systems are coupled the stochastic oscillations of the two subsystems rapidly phase synchronize. The temporal behavior of the two repressors for direct coupling is shown in Fig. 3.9 and exchange coupling in Fig. 3.10.

3.4 Circadian Oscillator with Time Delay

For spatially extended systems, it is necessary to include time delay in the interactions [34]. For instance, in the case of coupling of biochemical networks in different cells, intercellular diffusion must be taken into account [35]. In such situation as a function of delay time τ, the nature of synchronization can itself change, from being in phase to being antiphase (or out of phase);

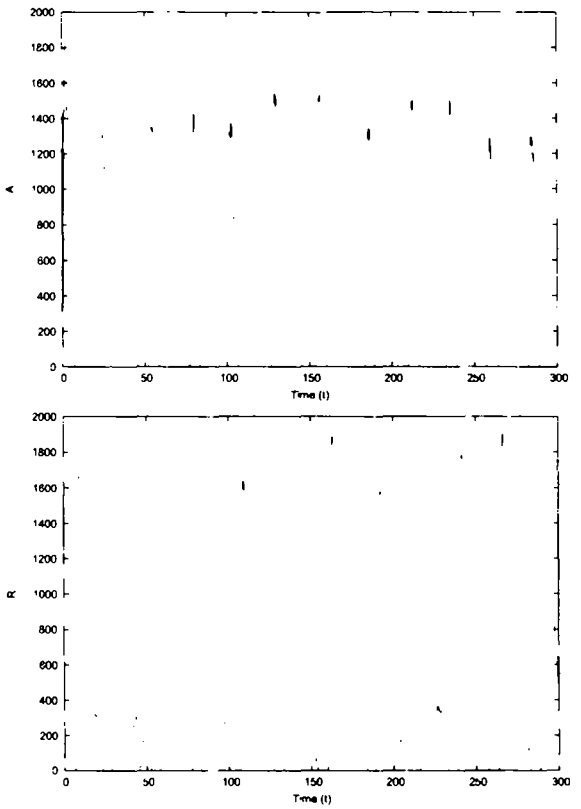

Figure 3.8: Oscillations in activator A and repressor R protein numbers obtained from numerical simulations of the stochastic descriptions of the model.

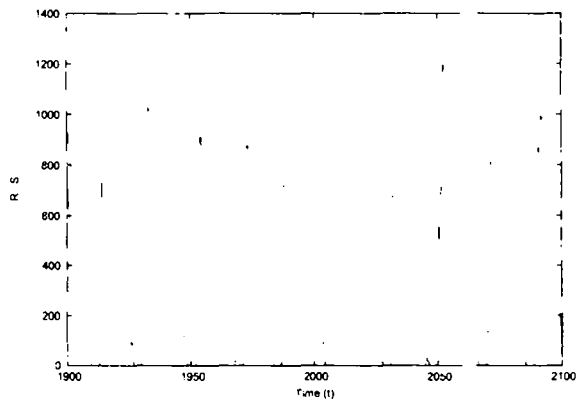

Figure 3.9: Temporal pattern when two circadian oscillators are coupled directly.

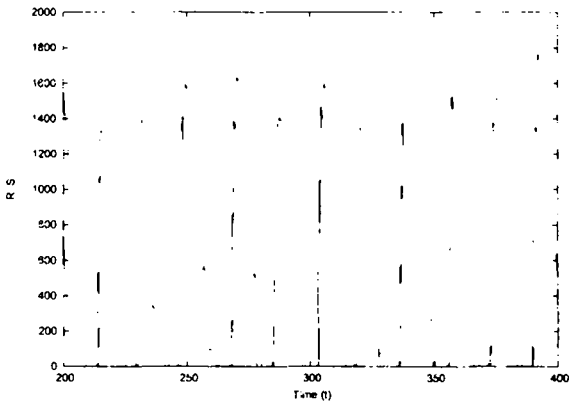

Figure 3.10: Temporal pattern when two circadian oscillators are coupled through exchange coupling with c=c'=0.55.

the Hilbert phase difference in the later case takes the value π rather than zero [30]. The time evolution of such systems can be studied through an appropriately adapted stochastic simulation technique [35, 29].

One can extend the exchange process to include time delay, namely [30]

$$\begin{aligned} X_i &\xrightarrow{c} X_i' \quad \text{with delay} \tau \\ X_i' &\xrightarrow{c'} X_i \quad \text{with delay} \tau \end{aligned} \tag{3.16}$$

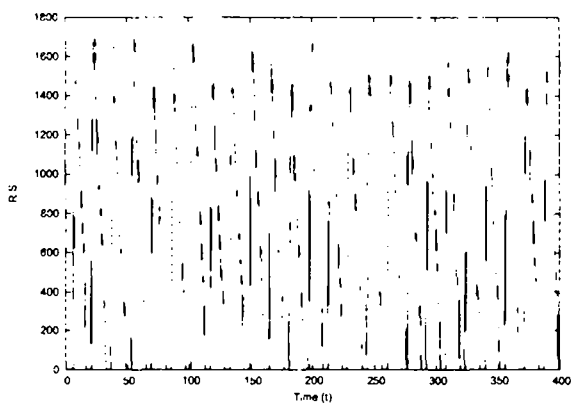

Figure 3.11: When the two circadian oscillators are coupled bidirectionally with time delay, the repressors R and S vary in phase. This phase synchrony is for time delay τ =15 and coupling strength c=c'=0.7.

Here I use a modified Gillespie Algorithm [29] which takes into account

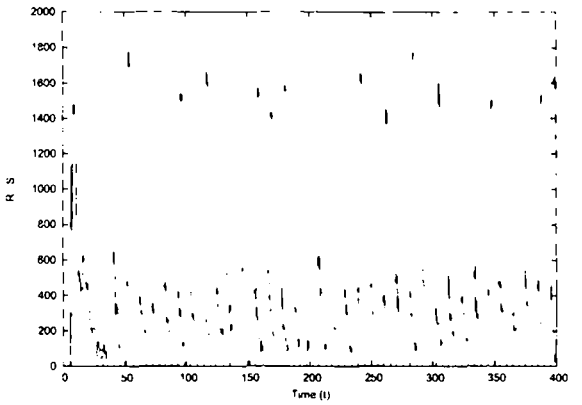

Figure 3.12: When the two circadian oscillators are coupled bidirectionally with time delay, the repressors R and S vary in anti phase. This anti phase synchrony is for time delay τ =10 and coupling strength c=c'=0.7

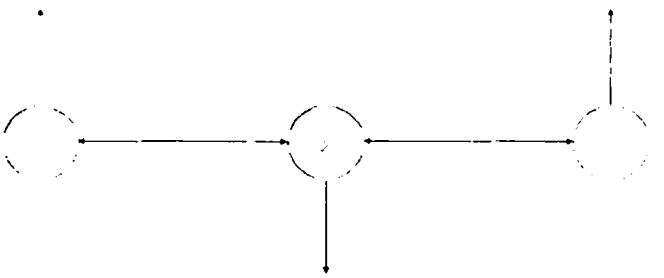

Figure 3.13: Schematic representation of the relay mechanism. There is no direct coupling between 1 and 3, 1 and 3 are coupled bidirectionally to oscillator 2.

the non Markovian nature of the dynamics when time delay is present. For appropriate combinations of delay time and exchange rate, circadian oscillator systems synchronize. The coupled oscillators also exhibit antiphase synchronization for specific combinations of (c, τ). which are shown in Fig. 3.11 and 3.12.

3.5 Relay Synchronization

The coupling topology which is shown in Fig. 3.13, when the two oscillators (denoted by 1 and 3) are time-delay diffusely coupled to a third oscillator (marked 2) is of special interest.

The three repressors from the three subsystems, labeled R, S, and T respectively, have the dynamics: oscillators denoted by 1 and 3 which are time -delay diffusely coupled to oscillator 2 show phase synchrony even if they are not directly coupled and all the parameters of the systems differ Fig. 3.14. For different combinations of delay time and coupling strength, one can find following regimes

- Oscillator 2 is out of phase with the outputs of oscillators 1 and 3 which are in phase.
- Oscillator 2 is antiphase to oscillators 1 and 3 which are in phase: Fig 3.15 and 3.16.

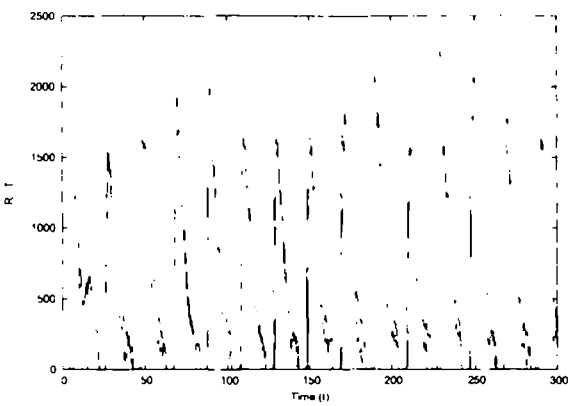

Figure 3.14: Relay Synchronization: oscillators 1 and 3 show phase synchrony, even if there is no direct coupling between 1 and 3, 1 and 3 are coupled bidirectionally to oscillator 2.

The above strategy is very powerful, in the sense that one can make arbitrary number of oscillators synchronize either in phase or out of phase by suitable coupling topology and the time delay [30].

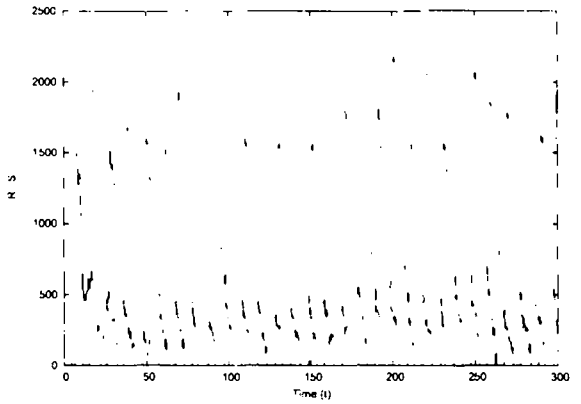

Figure 3.15: Relay Synchronization: oscillator 1 and 2 show antiphase synchronization.

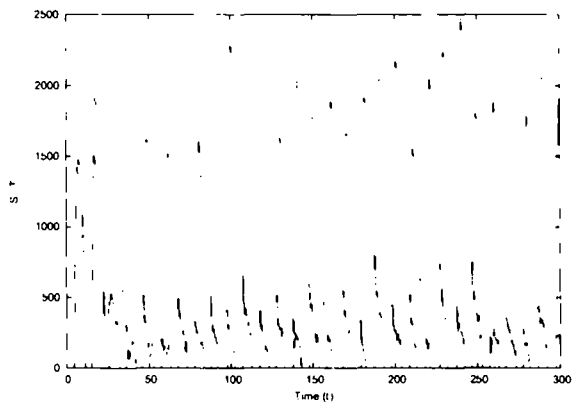

Figure 3.16: Relay Synchronization: oscillator 2 and 3 show antiphase synchronization .

3.6 Network Topology

Having discussed the coupling mechanisms by which two oscillator units can be synchronized, I consider extended systems composed of stochastic oscillators. When coupled on networks, such systems are of great current interest. Spatiotemporal patterns that emerge as a consequence of the complex network topology play a crucial role in determining cellular function.

It is useful to identify the simplest units of commonly used network architectures [36] in order to understand the manner in which complex networks function. It is believed that these network motifs provide the useful information of basic regulatory mechanism and hence these network motifs contribute

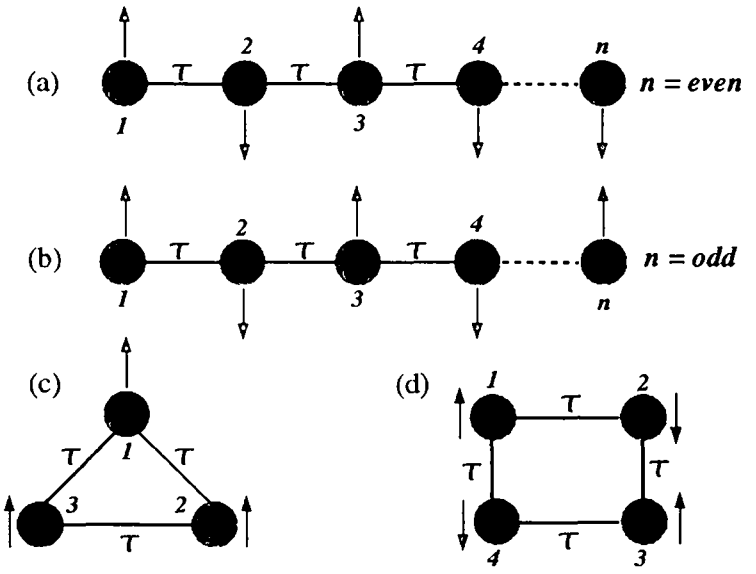

Figure 3.17: Different network motifs for oscillators coupled bi-directionally via delayed channels. (a) and (b) show one-dimensional open chains with even and odd number of nodes. (c) shows a triangle motif with identical delay times τ, and (d) shows a square motif. The arrows indicate the relative phases of the oscillators at the nodes.

in building complex temporal behavior. I study a set of stochastic oscillators coupled in a motif. The coupling incorporates delay and thus there is a possibility of relay synchronization. As a example I use the circadian oscillator system at each node; the nodes are coupled via the mechanisms discussed in relay synchronization, and we consider the resulting temporal patterns see Fig. 3.17.

3.6.1 Open Chain

The simplest motif is the one-dimensional open chain where oscillators are coupled sequentially. Depending upon the choice of τ and coupling strength, there could be several possibilities. If the time-delay is small in comparison with the intrinsic time-scale of oscillation, say then with increasing coupling strength all the oscillators get phase-synchronized. When the time-delay is

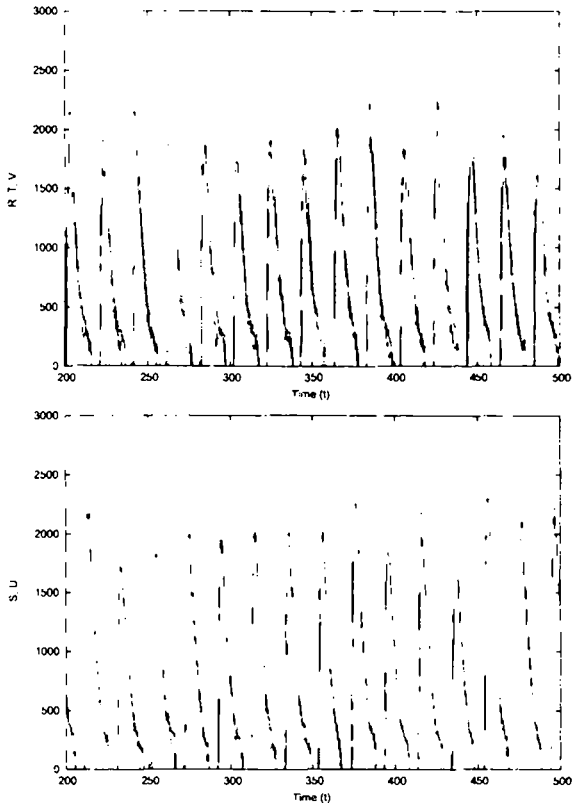

Figure 3.18: Phase synchronization of the circadian oscillators in an odd chain with $n = 5$, $\tau = 10$ and $c = 0.8$. In first, the repressors R, T and V of the oscillators 1, 3 and 5 are phase-synchronized, whereas in second fig. the repressors S and U of the oscillators 2 and 4 are in phase. The alternate oscillators are anti-phase-synchronized.

of the order of the characteristic time-scale of the system, alternate oscillators can become phase-synchronized while neighboring oscillators are lag-synchronized, a consequence of relay synchronization. With an even number of oscillators, oscillators at the end of the chains will necessarily be in lag synchrony, while if there is an odd number of oscillators they will be in phase. Fg. 3.18 shows one such situation with $n = 5$ where the oscillators 1, 3 and 5 are phase-synchronized.

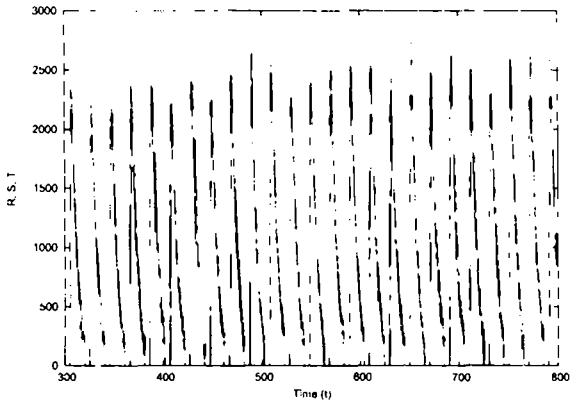

Figure 3.19: Circadian oscillators put in a triangular motif as in Fig. 3.17(c). Phase synchronization of the repressors is achieved when equal coupling strength and time-delay are used. Here $c = 0.9$ and $\tau = 20$.

3.6.2 Closed Chain

I also study closed chains.Three oscillators each coupled to the other results in triangular motif, of Fig. 3.17(c) or four oscillators coupled in a quadrilateral Fig. 3.17(d). For the shake of simplicity, I consider the case of equal time-delays. In case of equilateral triangle, node 2 acts as a relay between nodes 1 and 3. But node 3 can act as a relay between nodes 1 and 2 to get them in-phase. Thus there are two possibilities, due to these competing effects, depending on the coupling strength and time-delay, the synchronization can either be destroyed or all three become synchronized. In the case of square motif, no such competition arises and as before the alternate oscillators are phase synchronized. Therefore for systems coupled in a closed chain with odd number of nodes, it is possible to have all the oscillators phase synchronized. With even number of nodes, a closed chain behaves like an open chain.

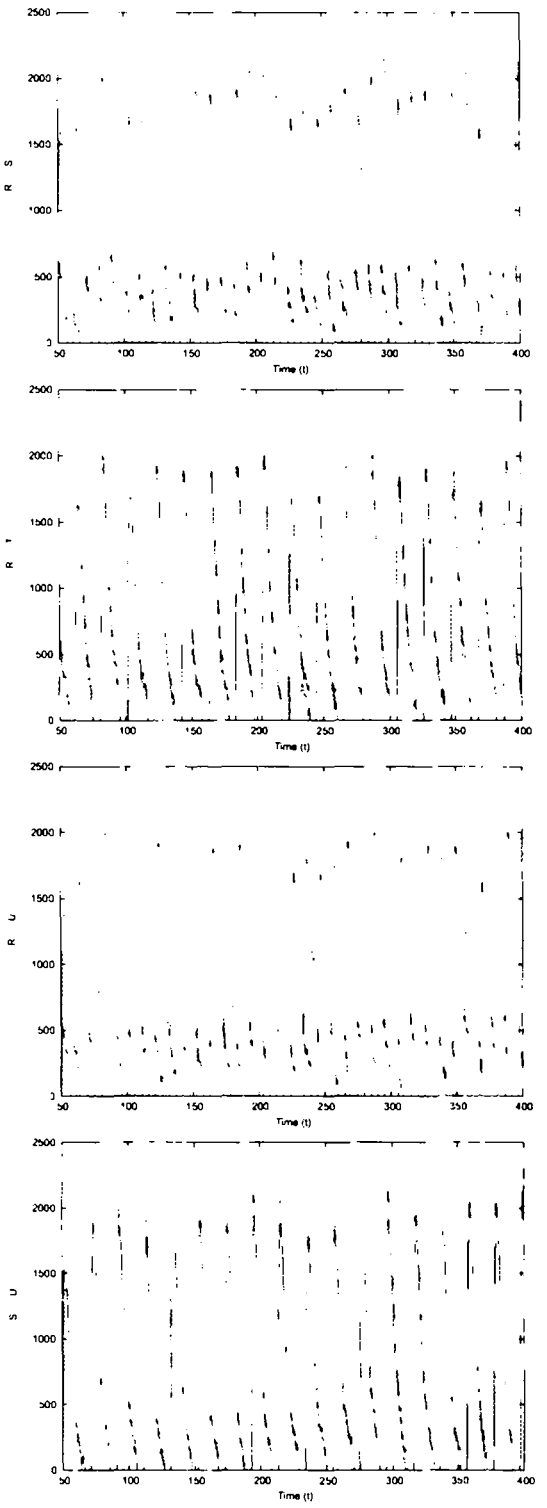

Figure 3.20: Circadian oscillators put in a square motif as in Fig. 3.17(d).

Chapter 4

Conclusion

In the present work I have explored temporal patterns of extended systems with stochastic dynamics, particularly the nature of synchronization, I have investigated some of the simplest mechanisms through which such synchrony can be effected, and using the idea of relay synchronization I have studied various network motif.

The microscopic behavior of typical transcriptional gene regulatory circuit, both as individual, and ensembles of such circuits have been explored. In the case of spatially extended systems, it is necessary to include time delay in the interactions. In such situations the nature of temporal patterns can change as a function of delay time τ and the nature of synchronization will be phase or antiphase or out of phase as a function of the coupling topology.

The coupling schemes which I have discussed in the present work have application in the design and control of the synthetic biological networks where synchronization of oscillations may be a desirable feature. McMillen et. al [37] have shown that intercell signaling via a diffusing molecule can couple genetic oscillators and effect synchrony. Phase synchrony can emerge under very general conditions with high level of ambient noise [30]. As recent time-resolved microarray experiments of yeast have revealed, the multitude of variable gene expression patterns classify into a small number of groups, all genes of a given group having very similar temporal variation profiles [38]. This may be a consequence of large scale synchronization.

Using the idea of relay synchronization, I have studied various network motifs, showing the possibility of achieving synchronization as well as complex temporal variations over large distances. This study will provide a framework within which one can study the various oscillatory processes within cells, and may also be useful in analyzing intercellular communication.

Bibliography

[1] U. Schibler and F. Naef,Current Opinion in Cell Biology **17**,223 (2005).

[2] M . B. Elowitz and S. Leibler, Nature **403**, 335 (2000).

[3] M . R. Atkinsion, M. A. Savageau, J. T. Myers and A. J. Ninfa, Cell **113**,597 (2003).

[4] E. Fung, W. W . Wong, J. K. Suen, T. Bulter, S. G. Lee and J. C. Liao, Nature **435**. 118 (2005).

[5] M. G. Vilar, H. Y. Kuech, N. Barkai, and S. Leibler, Proc. Natl. Acad. Sci. (USA) **99**, 5988 (2002).

[6] N. Barkai and S. Leibler, Nature **403**, 267 (2000).

[7] L. N. Edmunds *Cellular and Molecular Bases of Biological Clocks (Springer New York, 1998).*

[8] D. T. Gillespie, J. Phys. Chem. **81**, 25 (1977).

[9] C. V. Rao and A. P. Arkin, J. Chem. Phys. **118**, 4999 (2003).

[10] I. Goryanin, C. T. and E. Selkov, Bioinformatics **15**, 749 (1999).

[11] P. Mendes, Trends Biochem.Sci.**22**,361 (1997).

[12] Q. Dang and C. Frieden, Trends Biochem.Sci.**22**,317 (1997).

[13] M. Ehlde and G. Zachhi, Comput.Applic.Biosci. Biochem.Sci.**11**,201 (1995).

[14] B. Aleman-Meza, H. B. Schuttler, J. Arnold, T. R. Taha *http:/webster.cs.uga.edu/ boanerg/mams*

[15] E. O. Voit *Cambridge University Press, Cambridge, U K* 2000.

[16] M. Tomita, K. Hashimoto, K. Takahasi, T. Shimizu, Y. Matsuzaki, F. Miyoshi, K. Saito, S. Tanida, K. Yugi, J. Venter and C. A Hutchison, Bioinformatics **15**, 72 (1999).

[17] P. Dhar, C. M. Tan, S. Somani, Y. Li, A. Sairam, H. Zhu, M. Chitre and K. Sakharkar, Bioinformatics **20**, 1319 (2004)*www.webster.cs.uga.edu/ boanerg/mams.*

[18] D. A. McQuarrie, C. J. Jachimowski A and M. E. Russell, J. Chem. Phys. **40**, 2914 (1964).

[19] Q. Zheng and J. Ross, J. Chem. Phys. **173**, 6307 (1991).

[20] D. T. Gillespie, J. Chem. Phys. **113**, 1 (2000).

[21] D. T. Gillespie, Physica A **188**, 404 (1992).

[22] H. H. McAdams and A. Arkin, Trends Genet. **15**,65 (1999).

[23] D. T. Gillespie, J. Chem. Phys. **22**, 403 (1976).

[24] D. T. Gillespie, Annu.Rev.. Phys. Chem. **58**, 35 (2007).

[25] T. C. Meng, S. Somani and P. Dhar, In Sillico Biology **4**,24 (2004).

[26] M. A. Gibson and J. Bruck, J. Phys. Chem. **105**, 1876 (2000).

[27] D. T. Gillespie, J. Chem. Phys. **115**, 1716 (2001).

[28] D. T. Gillespie and L. R. Petzold, J. Chem. Phys. **119**, 8229 (2003).

[29] D. Bratsun, D. Volfson and J. Hasty, Proc. Natl. Acad. Sci. (USA) **102**, 41 (2005).

[30] A. Nandi, Santhosh G, B. Singh, R. Ramaswamy, Phys. Rev. E **76**, 41136 (2007).

[31] D. A . McQuarrie, J. Appl . Probab .**4**,413 (1967).

[32] I. Oppenheim, K. E. Schuler, and G. H. Weiss, Stochtic Processes in Chemical Physics: The Master Equation (MIT Press, Massachusetts) J. Appl . Probab .**4**,413 (1967).

[33] J. C Dunlap, Cell **96**,271 (1999).

[34] M. G. Rosenblum and A. S. Pikovsky, Phys. Rev. Lett. **92**, 114102 (2004).

[35] L. Chen, R. Wang, T. Zhou and K. Aihara, Bioinformatics **21**, 2722 (2005).

[36] T. I. Lee, Science **298**, 799 (2002).

[37] D. Mcmillen, N. Kopell, J. Hasty and J. J. Collins, Proc. Natl. Acad. Sci. (USA) **99**, 679 (2002).

[38] B . P. Tu, A. Kudlicki, M. Rowicka and S . L. McKnight, Science **310**, 1152 (2005).